

Wang, W. et al. (2013). Nanoparticle TiO₂-promoted PtRu/C catalyst for methanol oxidation: TiO₂ nanoparticles promoted PtRu/C catalyst for MOR. *Ionics*, 19: 592 – 534
<http://dx.doi.org/10.1007/s11581-012-0773-1>



Nanoparticulate TiO₂-promoted PtRu/C catalyst for methanol oxidation: TiO₂ nanoparticles promoted PtRu/C catalyst for MOR

Wei Wang, Hui Wang, Julian Key, Vladimir Linkov, Shan Ji and Rongfang Wang

Abstract

To improve the electrocatalytic properties of PtRu/C in methanol electrooxidation, nanoparticulate TiO₂-promoted PtRu/C catalysts were prepared by directly mixing TiO₂ nanoparticles with PtRu/C. Using cyclic voltammetry, it was found that the addition of 10 wt% TiO₂ nanoparticles can effectively improve the electrocatalytic activity and stability of the catalyst during methanol electro-oxidation. The value of the apparent activation energy (E_a) for TiO₂-PtRu/C was lower than that for pure PtRu/C at a potential range from 0.45 to 0.60 V. A synergistic effect between PtRu and TiO₂ nanoparticles is likely to facilitate the removal of CO-like intermediates from the surface of PtRu catalyst and reduce the poisoning of the PtRu catalysts during methanol electrooxidation. Therefore, we conclude that the direct introduction of TiO₂ nanoparticles into PtRu/C catalysts offers an improved facile method to enhance the electrocatalytic performance of PtRu/C catalyst in methanol electrooxidation.

Introduction

Carbon-supported PtRu catalyst, PtRu/C, offers a state-of-the-art anode electrocatalyst for direct methanol fuel cells (DMFCs) due to its high activity toward methanol electro-oxidation and tolerance to carbon monoxide poisoning [1–5]. Alloying Pt with Ru promotes the formation of oxygenated species at a lower temperature than Pt particles and promotes oxidation of CO to CO₂. However, despite promising progress in the development of PtRu/C, the durability and activity of the PtRu/C anode still cannot meet the demands for practical DMFCs applications.

Various metal oxides such as IrO₂, V₂O₅, WO₃, CeO₂, MoO₃, Nd₂O₃, RuO₂, and TiO₂ can enhance the catalytic activity of Pt-based electrocatalysts for methanol oxidation reaction (MOR) [6–15]. Among them, TiO₂ is the most promising promoter of PtRu/C due to its natural abundance, low cost, and stability in acidic environments [15–21]. The addition of TiO₂ to Pt-based catalysts can lower the adsorption energy of CO on the surface of Pt-based nanoparticles because TiO₂ is reduced to Ti⁺³, which results in a higher electronic density on Pt-based nanoparticles and in turn changes its chemisorption properties and weakens the bond between Pt and CO [16]. Various studies have introduced TiO₂ into Pt-

based electrocatalysts via hydrolysis of organic Ti sources, such as $\text{Ti}(\text{OBU})_4$ [15, 16, 18, 19]. However, the methods are quite complicated and unsuitable for large-scale production and furthermore do not allow for easy manipulation of the TiO_2 content and structure in the catalyst.

In this study, a facile way to prepare TiO_2 -modified PtRu/ C (TiO_2 -PtRu/C) has been successfully developed by directly introducing commercial TiO_2 nanoparticles into the preparation process of PtRu/C electrocatalysts. The electrocatalytic properties of TiO_2 -modified PtRu/C for MOR were evaluated by cyclic voltammetry and chronoamperometry, and the effect of temperature on MOR was also investigated. E_a calculated to evaluate the effects and mechanism of TiO_2 in the electrocatalytic activity of TiO_2 -PtRu/C in MOR.

Experimental

TiO_2 -PtRu/C catalysts were synthesized by a modified organic colloid method in an ethylene glycol (EG) solution. H_2PtCl_6 and RuCl_3 (atomic ratio of Pt to Ru is 1:1) were dissolved in 50 ml of EG in a flask. The pH of above solution was adjusted to 9 by 5 wt% of KOH/EG solution. Pretreated carbon black Vulcan® XG72R was added to the mixture with stirring and ultrasonicated for 1 h (PtRu/Co40:60). The mixture was transferred into a flask and heated at 160 °C for 6 h. Specific amounts of commercial TiO_2 (99.8 %, 5–10 nm, Aladdin Chemistry Co. Ltd) (ratios of PtRu to TiO_2 were 90:10, 80:20, 70:30, and 60:40) were introduced into the same above mixtures and ultrasonicated for 0.5 h. The synthesized TiO_2 -PtRu/C catalysts were collected by filtration and washed with deionized water to remove chloride anions from the filtrate. The products were dried in air at 60 °C for 12 h.

Electrochemical studies on the catalysts used an Autolab electrochemical workstation (PGSTAT128N). A common three-electrode electrochemical cell was used for the measurements. The counter and reference electrodes were a platinum wire and an Ag/AgCl (3 M KCl) electrode, respectively. The working electrode was a 5-mm diameter glassy carbon disk. The thin film electrode was prepared as follows: 5 mg of catalyst was dispersed ultrasonically in 1 mL Nafion/ethanol (0.25 % Nafion) for 15 min. Eight microliters of the dispersion was transferred onto the glassy carbon disk using a pipette and then dried in the air. The catalysts were characterized by cyclic voltammetry (CV) and chronoamperometry tests at room temperature. Before each measurement, the solution was purged with high purity N_2 gas for at least 30 min to ensure O_2 Results and discussion The electrocatalytic activities of PtRu/C and TiO_2 -PtRu/C catalysts toward MOR were investigated by cyclic voltammetry in CH_3OH 0.5 M + H_2SO_4 0.5 M solution. The mass activity of precious metal for MOR is a critical parameter in terms of its practical applications. The activity measurement results based on the total PtRu mass are shown in Fig. 1. The mass activity of the TiO_2 -PtRu/C (10 %) and TiO_2 -PtRu/C (5 %) catalyst was 0.20 and 0.19 Amg^{-1} PtRu, respectively, which was higher than that of PtRu/C catalyst (0.18 Amg^{-1} PtRu). Additionally, the onset potential for the TiO_2 -PtRu/C (10 %) and TiO_2 -PtRu/C (5 %) catalyst was also lower than that of PtRu/C.

Therefore, MOR activity of PtRu/C is promoted by introducing TiO₂ nanoparticles into PtRu/C. The proposed reason for this improvement is that on TiO₂-PtRu/C, OH species can easily form on the surface of TiO₂ during the MOR process, which facilitates the conversion of the poisonous CO into CO₂ [22].

The amount of TiO₂ nanoparticles in the PtRu/C catalyst had a significant effect on the activity towards MOR. Further increase of TiO₂ content (20, 30, and 40 %) resulted in the reduction of current value. This phenomenon can be explained by a percolation effect, which is also observed when Fe₂O₃ nanoparticles are introduced into PtRu/C catalysts [14]; too much TiO₂ can block the path of electron transportation to the PtRu catalyst. Additionally, when the TiO₂ nanoparticles content increases, the oxophilicity also increases which leads to a decrease in the activity because the OH groups on these particles can effectively block the active sites required for the adsorption of CH₃OH [23].

Since the MOR activity of PtRu/C was improved by mixing certain amount of TiO₂ nanoparticles (10 wt%), the property of the TiO₂-PtRu/C (10 wt%) catalyst was further investigated and compared with the PtRu/C catalyst. Figure 2 shows the cyclic voltammetric curves in N₂-purged 0.5 M H₂SO₄ electrolyte, recorded on PtRu/C and TiO₂-PtRu/C (10 wt%) catalysts from -0.2 to 1 V (vs. Ag/AgCl). Both catalysts had the characteristic features of polycrystalline Pt, i.e., hydrogen adsorption/desorption peaks in low potential region, oxide formation/stripping wave/peak in high potential region, and a flat double layer in between. Compared with the CV curves of PtRu/C and TiO₂-PtRu/C, the double layer regions of TiO₂-PtRu/C are thicker than that of PtRu/C catalyst, which may be caused by the OH species absorbed on the surface of TiO₂ nanoparticles.

The electrochemically active specific area (SEAS) was also obtained from CO-stripping voltammetry carried out in 0.5 M H₂SO₄ at a scan rate of 50 mV s⁻¹ at room temperature.

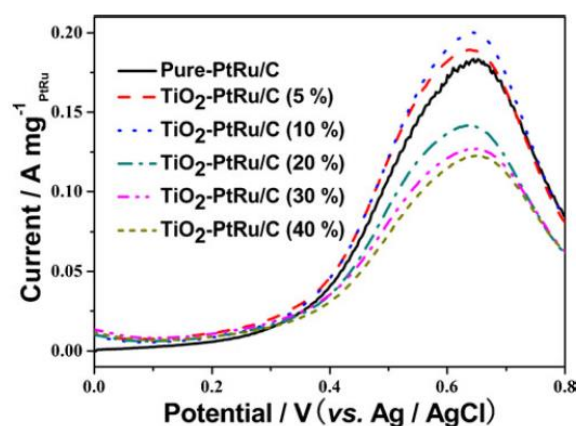


Fig. 1 Cyclic voltammograms of the PtRu/C and TiO₂-PtRu/C catalyst with various amounts of TiO₂ in 0.5 M CH₃OH+0.5 M H₂SO₄ solution under N₂ atmosphere. Scan rate, 50 mV s⁻¹; at room temperature. Rotation speed, 300 rpm

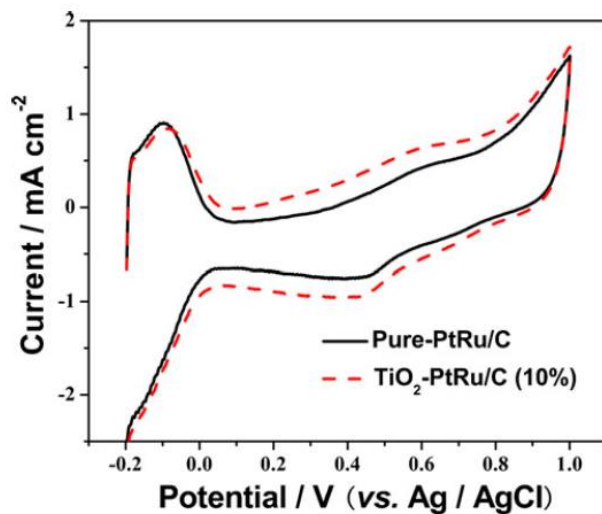


Fig. 2 Cyclic voltammograms of PtRu/C and TiO₂-PtRu/C (10 %) catalysts in 0.5 M H₂SO₄ under N₂ atmosphere; scan rate, 50 mV s⁻¹, at room temperature. Rotation speed, 300 rpm

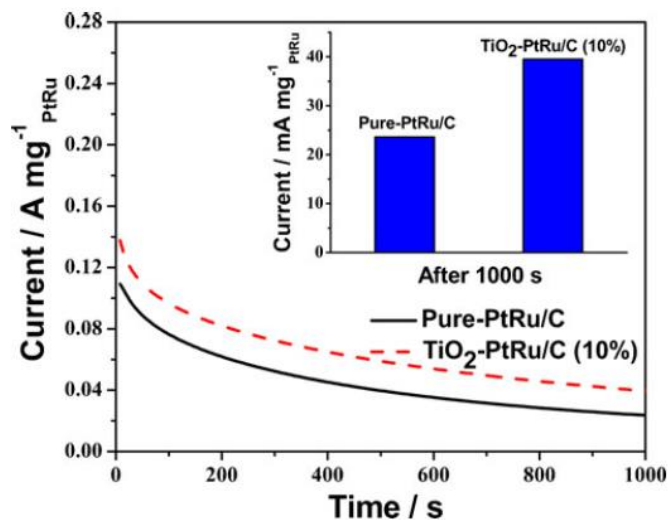


Fig. 3 The chronoamperometric curves of 0.5 M CH₃OH+0.5 M H₂SO₄ solution on PtRu/C and TiO₂-PtRu/C (10 %) catalysts for 1,000 s at room temperature. Fixed potential, 0.6 V; rotation speed, 300 rpm. *Inset*: the current of catalysts after 1,000 s

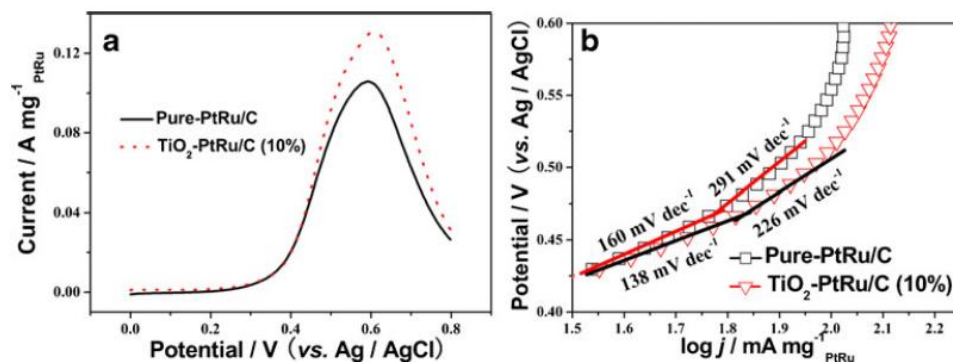
The $SEAS$ of the catalysts was calculated by using the equation [24], $SEAS = QCO/420\delta\mu C \text{ cm}^{-2}P=w$, where $SEAS$ is the electrochemically active specific area of different catalysts; QCO is the charge for CO desorption electrooxidation in microcoulomb (μC); 420 is the charge required to oxidize a monolayer of CO on the catalyst in microcoulomb per square centimeter, and w is the Pt loading. The $SEAS$ of the PtRu/C and TiO₂-PtRu/C (10 %) catalysts is 75.70 and 80.08 $\text{m}^2 \text{ g}^{-1} \text{ Pt}$, respectively, similar to the literature [25]. The $SEAS$ of TiO₂-PtRu/C is slightly larger than that of PtRu/C, which may be due to the formation of new sites at the interface between the platinum and the oxide materials. The chronoamperometry measurement provides further information about the electroactivity and stability of the catalysts for MOR. Chronoamperograms in 0.5 M H₂SO₄ + 0.5 M CH₃OH are shown in Fig. 3, in which the mass is also based on the total PtRu mass. In the initial stage, all potentiostatic currents decreased rapidly, corresponding to the formation of intermediate species such as CO_{ads}, CH₃OH_{ads}, and CHO_{ads} during the methanol oxidation reaction [26]. Figure 3 shows that the current density of TiO₂-PtRu/C (10 %) is higher than that of PtRu/C. The current on PtRu/C and TiO₂-PtRu/C (10–1wt%) catalysts after 1,000 s was 23.6 and 39.7 mA mgPtRu, respectively. A cooperative effect of Pt with TiO₂ nanoparticles can accelerate the oxidation of absorbed CO-like intermediate species [27], which in turn improve the stability of the TiO₂-PtRu/C (10 wt%) catalyst for MOR. Ru is known to be dissolved or dealloyed from PtRu alloy particles, which will result in the activity loss. It was reported that the presence of TiO₂ can restrain the Ru loss. The dissolved Ru species may be trapped on the surface of TiO₂ nanoparticles, preventing dissolved Ru from diffusion into the electrolyte, which should be beneficial to the stability of the TiO₂-PtRu/C (10 %) catalyst [15].

Figure 4a shows a typical linear sweep with a scan rate of 5 mV s^{-1} , which is close to a steady-state polarization curve of the MOR on PtRu/C and TiO₂-PtRu/C (10 wt%). Excellent linear correlations are found in both Tafel plots of PtRu/C and TiO₂-PtRu/C (10 wt%). In the low potential region, the current densities increased very slowly with increasing polarization potential and two curves are almost overlapped. In the relatively high potential region (above 0.45 V vs. Ag/AgCl), the polarization current increases sharply with polarization potential and the current density of the TiO₂-PtRu/C (10 %) catalyst is larger than those of PtRu/C catalysts. There is a limit current at about 0.6 V in Fig. 4a, which can be attributed to the blocking of active catalytic sites by the adsorbed intermediate species [28, 29].

Figure 4b shows the corresponding Tafel plot of the MOR, calculated from the quasi-steady-state curve in Fig. 4a. Each plot can be fitted and divided into two linear regions according to the change of Tafel slopes. The first fitted Tafel slopes fall within the scope of 138–160 mV dec^{-1} at low overpotentials (<0.45 V vs. Ag/AgCl), while the second slopes are in the range of 226–291 mV dec^{-1} at high overpotentials (0.45 to 0.50 V vs. Ag/AgCl). With increasing potential, the adsorbed CO-like residues are gradually oxidized, and thus, the active sites on platinum are cleaned up for the subsequent methanol dehydrogenation

reaction. So, the increase of the second Tafel slope is caused by the decreased coverage of the poisonous intermediate species [29]. The second slopes are almost twice higher than the first slopes, indicating a possible change of reaction mechanism or at least a transformation of rate-determining step at different potential range [29].

Fig. 4 Tafel plots of MOR on the PtRu/C and TiO₂-PtRu/C (10 %) in 0.5 M CH₃OH+ 0.5 M H₂SO₄ solution under N₂ atmosphere at room temperature. Scan rate, 5 mV s⁻¹



MOR on PtRu/C (Fig. 5a) and TiO₂-PtRu/C (10 wt%) (Fig. 5b) electrocatalyst were carried out at different temperatures between 10 and 40 °C in 0.5 M H₂SO₄ + 0.5 M CH₃OH solution. The corresponding cyclic voltammograms displayed an increasing oxidation current with rising temperature. As expected, the process of MOR is thermally activated. With temperature increasing, the current peak becomes stronger and the onset potentials shift to a lower position. The enhanced reaction rate occurs because the elevated temperature not only activates the C–H bond scission process but also accelerates the oxidation reaction of CO-like residues [29].

In many of these temperature-dependent MOR studies, apparent activation energies have been calculated. The apparent activation energies for MOR on the PtRu/C and TiO₂-PtRu/C (10 wt%) catalysts were obtained at different potentials by linear regression of the Arrhenius plots presented in Fig. 5c, d. Arrhenius plots for the two catalysts at different overpotentials are obtained by constructing diagrams of log *i* vs. reciprocal *T*, where *i* is the current density at controlled potentials and *T* is the applied temperature. The activation energies were calculated using the following equation [30]: $\log i \sim \text{const} - E_a/RT$, (where *i* is the current at a specific potential, *R* is the gas constant, *T* is the temperature in Kelvin, and *E_a* is the apparent activation energy at a specific potential) at a given potential.

Parameters, such as surface adsorption and poisoning, have a significant effect on the *E_a* value. Comparison of *E_a* values is an efficient way to evaluate the difference between two catalysts. The values of the activation energy are plotted vs. the potential in Fig. 6. *E_a* is potential dependent because a number of different surface processes and adsorption processes that affect the current values are potential dependent [30].

Fig. 5 Cyclic voltammetry of PtRu/C (a) and TiO₂-PtRu/C (10 %) (b) catalysts in 0.5 M CH₃OH+0.5 M H₂SO₄ solution under N₂ atmosphere within the temperature range of 10–40 °C; scan rate, 50 mV s⁻¹. Arrhenius plots of MOR on PtRu/C (c) and TiO₂-PtRu/C (10 %) catalysts (d)

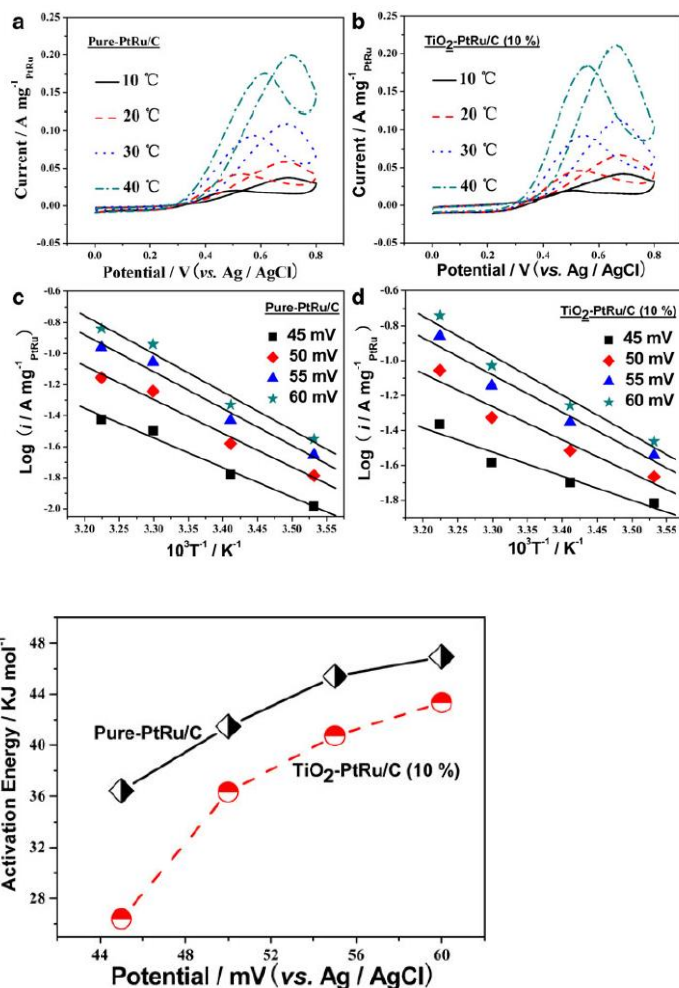


Fig. 6 Apparent activation energy vs. potentials

The activation energy values obtained on PtRu/C and TiO₂-PtRu/C (10 wt%) catalysts under potential from 0.45 to 0.60 V range from 36.4 to 46.9 kJ mol⁻¹ and 26.4 to 43.3 kJ mol⁻¹, respectively. This correlates with previously reported values for MOR on PtRu catalysts varying from 29 to 70 kJ mol⁻¹ sharing both a similar preparation method and working conditions [29]. The value of apparent activation energy of TiO₂-PtRu/C (10 wt%) is lower than that of PtRu/C over the whole potential range, which results from the synergistic effect of PtRu and TiO₂ nanoparticles. Similar to Pt catalyst, the OH species, which are present on the surface of TiO₂ in aqueous solutions, cause a greater shift in the surface oxidation of Pt (Pt–OH formation). Therefore, the presence of TiO₂ facilitates the removal of CO-like intermediates from the surface of PtRu catalyst and reduces the poisoning of the PtRu catalysts during MOR [22].

Conclusions

TiO₂-modified PtRu/C catalysts with various TiO₂ contents were successfully prepared via a facile method of directly adding TiO₂ nanoparticles into PtRu/C catalysts. The results show that this method of adding TiO₂ in PtRu/C catalysts can improve the

electrocatalytic performance in MOR. The value of the apparent activation energy of TiO₂-PtRu/C (10 wt%) is lower than that of PtRu/C over the whole potential range due to the synergistic effect between PtRu and TiO₂ nanoparticles, which facilitates the removal of CO-like intermediates from the surface of PtRu catalyst and reduces poisoning of the PtRu catalysts during MOR. Therefore, we conclude that directly introducing TiO₂ nanoparticles into PtRu/C catalysts offers an improved facile method for improving the electrocatalytic performance of PtRu/C catalyst in MOR.

Acknowledgments

We gratefully acknowledge the National Natural Science Foundation of China (21163018), the National Science Foundation for Post-Doctoral Scientists of China (20110490847), and the South African NRF (SUR 2008060900021) for financially supporting this work.

References

1. Wang YJ, Wilkinson DP, Zhang JJ (2011) Noncarbon support materials for polymer electrolyte membrane fuel cell electrocatalysts. *Chem Rev* 111:7625–7651
2. Li JH, Fan LZ, Liao LB (2010) Electrodeposition of platinum on tourmaline and application as an electrocatalyst for oxidation of methanol. *Ionics* 16:33–38
3. Zhou WJ, Zhou ZH, Song SQ, Li WZ, Sun GQ, Tsiakaras P, Xin Q (2003) Pt based anode catalysts for direct ethanol fuel cells. *Appl Catal B-Environ* 46:273–285
4. Brandalise M, Verjullo-Silva RWR, Tusi MM, Correa OV, Farias LA, Linardi M, Spinacé EV, Oliveira Neto A (2009) Electro-oxidation of ethanol using PtRuBi/C electrocatalyst prepared by borohydride reduction. *Ionics* 15:743–747
5. Huang T, Liu JJ, Li RS, Cai WB, Yu AS (2009) A novel route for preparation of PtRuMe (Me=Fe, Co, Ni) and their catalytic performance for methanol electrooxidation. *Electrochem Commun* 11:643–646
6. Zhang YN, Zhang HM, Ma YW, Cheng JB, Zhong HX, Song SD, Ma HP (2010) A novel bifunctional electrocatalyst for unitized regenerative fuel cell. *J Power Sources* 195:142–145
7. Maiyalagan T, Khan FN (2008) Electrochemical oxidation of methanol on Pt/V₂O₅-C composite catalysts. *Catal Commun* 10:433–436
8. Scibioh MA, Kim SK, Cho EA, Lim TH, Hong SA, Ha HY (2008) Pt-CeO₂/C anode catalyst for direct methanol fuel cells. *Appl Catal B-Environ* 84:773–782
9. Micoud F, Maillard F, Gourgaud A, Chatenet M (2009) Unique CO-tolerance of Pt-WO_x materials. *Electrochem Commun* 11:651–654
10. Huang T, Zhang D, Xue L, Cai WB, Yu A (2009) A facile method to synthesize well-dispersed PtRuMoO_x and PtRuWO_x and their electrocatalytic activities for methanol oxidation. *J Power Sources* 192:285–290
11. Justin P, Ranga Rao G (2011) Methanol oxidation on MoO₃ promoted Pt/C electrocatalyst. *Int J Hydrogen Energy* 36:5875–5884
12. Cao L, Scheiba F, Roth C, Schweiger F, Cremers C, Stimming U, Fuess H, Chen L, Zhu W, Qiu X (2006) Novel nanocomposite Pt/RuO₂·xH₂O/carbon nanotube catalysts for direct methanol fuel cells. *Angew Chem Int Ed* 45:5315–5319
13. Chen L, Guo M, Zhang HF, Wang XD (2006) Characterization and electrocatalytic properties of PtRu/C catalysts prepared by impregnation-reduction method using Nd₂O₃ as dispersing reagent. *Electrochim Acta* 52:1191–1198
14. Jeon MK, Lee KR, Woo SI (2010) Enhancement in electro-oxidation of methanol over PtRu black catalyst through strong interaction with iron oxide nanocluster. *Langmuir* 26:16529–16533
15. Saida T, Ogiwara N, Takasu Y, Sugimoto W (2010) Titanium oxide nanosheet modified PtRu/C electrocatalyst for direct methanol fuel cell anodes. *J Phys Chem C* 114:13390–13396
16. Yoo SJ, Jeon TY, CYH, Lee KS, Sung YE (2010) Particle size effects of PtRu nanoparticles embedded in TiO₂ on methanol electrooxidation. *Electrochim Acta* 55:7939–7944
17. Hepel M, Dela I, Hepel T, Luo J, Zhong CJ (2007) Novel dynamic effects in electrocatalysis of methanol oxidation on supported nanoporous TiO₂ bimetallic nanocatalysts. *Electrochim Acta* 52:5529–5547

18. Wang Z, Chen G, Xia D, Zhang L (2008) Studies on the electrocatalytic properties of PtRu/C-TiO₂ toward the oxidation of methanol. *J Alloy Compd* 450:148–151
19. Tian J, Sun G, Jiang YS, Mao Q, Xin Q (2007) Highly stable PtRuTiO_x/C anode electrocatalyst for direct methanol fuel cells. *Electrochem Commun* 9:563–568
20. Jiang ZZ, Wang ZB, Chu YY, Gu DM, Yin GP (2011) Ultrahigh stable carbon riveted Pt/TiO₂-C catalyst prepared by in situ carbonized glucose for proton exchange membrane fuel cell. *Energy Environ Sci* 4:728–735
21. Shanmugam S, Gedanken A (2007) Carbon-coated anatase TiO₂ nanocomposite as a high-performance electrocatalyst support. *Small* 3:1189–1193
22. Yoo SJ, Jeon TY, Lee KS, Park KW, Sung YE (2010) Effects of particle size on surface electronic and electrocatalytic properties of Pt/TiO₂ nanocatalysts. *Chem Commun* 46:794–796
23. Fuentes S, Figueras F (1978) Hydrogenolysis of cyclopentane and hydrogenation of benzene on palladium catalysts of widely varying dispersion. *J Chem Soc, Faraday Trans* 74:174–181
24. Zhao Y, Yang X, Tian J, Wang F, Zhan L (2010) A facile and novel approach toward synthetic polypyrrole oligomers functionalization of multi-walled carbon nanotubes as PtRu catalyst support for methanol electro-oxidation. *J Power Sources* 195:4634–4640
25. Shim J, Lee CR, Lee HK, Lee JS, Cairns EJ (2001) Electrochemical characteristics of Pt-WO₃/C and Pt-TiO₂/C electrocatalysts in a polymer electrolyte fuel cell. *J Power Sources* 102:172–177
26. Kabbabi A, Faure R, Durand R, Beden B, Hahn F, Leger JM, Lamy C (1998) In situ FTIRS study of the electrocatalytic oxidation of carbon monoxide and methanol at platinum–ruthenium bulk alloy electrodes. *J Electroanal Chem* 444:41–53
27. Liu JH, Yu CB, Wang YJ, Xing W, Lu TH (2003) Studies on electrocatalytic performance of titanium oxide electrode modified with Pt toward oxidation of CO. *Chem J Chin U* 24:2263–2267
28. Gojkovic SL, Vidakovic TR, Urovic DR (2003) Kinetic study of methanol oxidation on carbon-supported PtRu electrocatalyst. *Electrochim Acta* 48:3607–3614
29. Zhu J, Cheng F, Tao Z, Chen J (2008) Electrocatalytic methanol oxidation of Pt_{0.5}Ru_{0.5}xSn_x/C (x 0.0–0.5). *J Phys Chem C* 112:6337–6345
30. Cohen JL, Volpe DJ, Abruna HD (2007) Electrochemical determination of activation energies for methanol oxidation on polycrystalline platinum in acidic and alkaline electrolytes. *Phys Chem Chem Phys* 9:49–77